Plasmonic bandgap formation in two-dimensional periodic arrangements of gold patches with subwavelength gaps

Roberto Marani,[1] Marco Grande,[1] Valeria Marrocco,[1] Antonella D'Orazio,[1,*] Vincenzo Petruzzelli,[1] Maria A. Vincenti,[2] and Domenico de Ceglia[2]

[1]*Dipartimento di Elettrotecnica ed Elettronica (DEE), Politecnico di Bari, via Re David 200, 70125 Bari, Italy*

[2]*Aegis Technologies Group, Inc., 410 Jan Davis Drive, Huntsville, Alabama 35806, USA*

**Corresponding author: dorazio@poliba.it*

Received November 2, 2010; revised January 18, 2011; accepted February 16, 2011; posted February 18, 2011 (Doc. ID 137595); published March 9, 2011

We report on the formation of plasmonic bandgaps in two-dimensional periodic arrangements of gold patches. Orthogonal arrays of subwavelength slits with different periodicities have been studied by means of a three-dimensional finite-difference time-domain (FDTD) code, changing incident polarization and geometrical parameters. Spectral response of gold patches having different a form factor and surrounded by different media have been also investigated and compared in order to give a full description of bandgap shifts paving the way for the design of polarization-sensitive devices. © 2011 Optical Society of America

OCIS codes: 240.6680, 050.6624, 050.1220.

In the last few years, several efforts have been devoted to the engineering of metal structures providing new efficient designs of devices for different applications such as sensing [1], beam steering [2], and photovoltaics [3]. Periodicity of one- and two-dimensional (2D) metal gratings has been demonstrated to provide an extremely powerful means to control light propagation and, as a consequence, to engineer the spectral response. Transmission and reflection properties of metal films comprising arrays of subwavelength apertures have been studied since Ebbesen *et al.* [4] experimentally proved that coupling of surface plasmons (SPs) through metal gratings gives rise to unexpected enhanced transmission phenomena. After this seminal work, the same peculiar mechanism has been observed in different nanopatterns, such as slits, where the excitation of guided modes allows coupling of light also below the theoretical diffraction limit [5,6].

Although numerous theoretical and experimental studies report on the optical response of metal gratings patterned with subwavelength slits [7–9], the effects of index-mismatched interfaces on transmission properties of 2D orthogonal arrangements of slits are still not fully understood. Our effort in this Letter is to shed light on the coupling phenomena between Fabry–Perot (FP) resonant modes and SPs on the metal grating under different excitation conditions for both freestanding and supported metal gratings. Moreover, a three-dimensional analysis of polarization dependence of the spectral response on geometrical parameters will be performed to point out the novel capability of such structures to be used in polarization-sensitive devices.

The system under investigation is sketched in the inset of Fig. 1. It comprises a 2D periodic arrangement of gold patches, whose sizes are l_x and l_y in the xy plane, and w is the thickness along the z axis; a is the gap between two adjacent patches, equal to 60 nm hereinafter, while p_x and p_y are the periodicities in the x and y direction, respectively. Gold permittivity $\varepsilon_m(\lambda)$ [10] has been fitted using a Drude dispersive model (for free electrons) and two Lorentz-like oscillators (for bound electrons). The gold model in the range of wavelengths between 400 and 1000 nm is reported in [11]. All the simulations have been performed using a three-dimensional FDTD code [12]. With reference to the inset of Fig. 1, periodic boundary conditions are applied to the elementary cell of the structure in the xy plane, whereas perfectly matched layers are used at the boundaries of the computational domain along the z axis. A plane wave arises from a total field/scattered field section placed 300 nm above the structure and impinges orthogonally on the periodic arrangement of gold patches. The sinusoidal input pulse (central wavelength equal to 700 nm) is modulated by a time-dependent Gaussian function 2.5 fs in width, centered at 100 fs, and linearly polarized with an angle θ with respect to the x axis. The elementary cell of the array has been sampled with a cubic grid step of 4 nm.

Figure 1 reports the spectral analysis of three square gold patch arrays having $p_x = p_y = 300$ nm and $w = 200$ nm in a wavelength range between 400 and 1000 nm. A periodicity equal to 300 nm allows only the observation of the zero-order transmission, which exhibits different

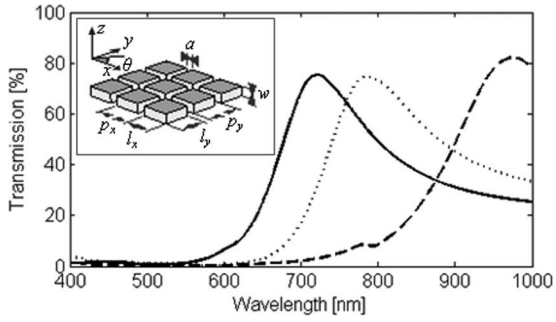

Fig. 1. Transmission spectra of the 2D array of metal patches as a function of the surrounding media: air (solid curve), SiO_2 (dashed curve), and semi-infinite substrate of SiO_2 (dotted curve). Geometrical parameters of the arrays are $p_x = p_y = 300$ nm, $a = 60$ nm, and $w = 200$ nm. Inset, sketch of the metal structure under investigation; θ is the angle between the x axis and the polarization vector of the impinging source.

values of resonances (see Fig. 1) when the surrounding material is homogeneous, air (solid curve) or silicon dioxide (SiO_2, dashed curve), and in the case of an asymmetric configuration with an air cover layer and a SiO_2 substrate (dotted curve). This structure resembles a system of FP cavities for the transverse-electromagnetic (TEM)-like guided modes excited in the slits. In this case the reflectance of the mirrors is related to the coupling of the TEM-like guided mode with the outer space. The spectral position of the transmission resonances of these cavities usually occurs when $w = \frac{m\lambda_0}{2n_{\text{eff}}}$, where m is an integer and n_{eff} is the effective index of the plasmonic metal–air–metal waveguide formed by each slit. The undisturbed FP-like resonances do not undergo any modulation effects due to surface waves excited in arrays since the periodicity is shorter than the impinging wavelength. On the other hand, these modulation effects become prominent when p_x and p_y are comparable to the FP resonant wavelengths (between 600 and 800 nm).

Figure 2 reports transmission and reflection diagrams of a freestanding array of gold patches, 200 nm thick, with $p_x = p_y = 600\,\text{nm}$ and $p_x = p_y = 800\,\text{nm}$. In this case, a minimum of transmission at normal incidence occurs at the wavelength $\lambda_{\min}$ where the unperturbed surface plasmon polariton (SPP) matches the grating periodicity. If the gap size is small enough to consider the input and output interfaces virtually smooth, the SPP would propagate almost undisturbed. Thus, counterpropagating leaky modes form a standing wave on the air–metal interface that reradiate backward, showing a spectral behavior that resembles a plasmonic bandgap reflector. Analytically, under normal incidence, we find $\lambda_{\text{spp}} = p_x$, and thus

$$\lambda_{\min} = p_x \sqrt{\frac{\varepsilon_d \varepsilon_m(\lambda_{\min})}{\varepsilon_d + \varepsilon_m(\lambda_{\min})}}, \tag{1}$$

where ε_d is the dielectric permittivity of the background medium. We find $\lambda_{\min} = 622.6\,\text{nm}$ when $p_x = p_y = 600\,\text{nm}$, and $\lambda_{\min} = 821.4\,\text{nm}$ when $p_x = p_y = 800\,\text{nm}$.

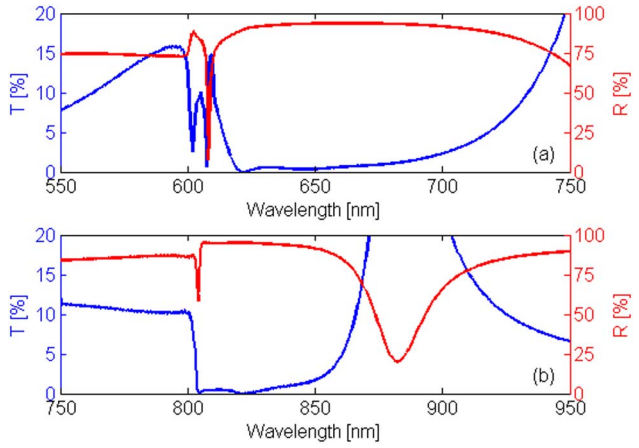

Fig. 2. (Color online) Transmission (blue curve) and reflection (red curve) diagrams for a structure comprising a squared array of freestanding patches with (a) $p_x = p_y = 600\,\text{nm}$, $a = 60\,\text{nm}$, and $w = 200\,\text{nm}$; and (b) $p_x = p_y = 800\,\text{nm}$, $a = 60\,\text{nm}$, and $w = 200\,\text{nm}$.

Furthermore, an accurate description of the dependence of transmission and reflection diagrams on the variation of the polarization angle θ is performed on the previous structure to prove that the squared array of gold patches does not exhibit any change in the spectral response, thus finding a perfect superposition of profiles on the diagram already shown in Fig. 2. This behavior can be explained by decoupling the incident electric field in two components along the x and y direction. Since each component experiences the same periodicity $p_x = p_y$, their recombination does not alter the spectral response of the squared array of patches regardless θ. To further prove that the two periodicities are actually acting independently, we consider an array with patches having a rectangular form factor. Figure 3 reports transmission and reflection diagrams as a function of θ, ranging from 0 to $\pi/2$, for a freestanding array of gold patches featuring $p_x = 600\,\text{nm}$ and $p_y = 800\,\text{nm}$. This analysis clearly demonstrates that the spectral response gradually changes between two different borderline cases corresponding to the matching conditions between the unperturbed SPP wavelength and the two periodicities, p_x and p_y.

We then move to the spectral analysis of these structures in a more realistic scenario, where a SiO_2 substrate supports the metal array. We started this study considering the polarization-insensitive square array of gold patches with $p_x = p_y = 600\,\text{nm}$, having a metal thickness equal to 200 nm. Figure 4 shows transmission (solid curve) and reflection (dashed curve) for a freestanding array [Fig. 4(a)], for a patch array embedded in SiO_2 [Fig. 4(b)], and placed over a semi-infinite SiO_2 substrate [Fig. 4(c)]. In the case of homogeneous background media [see Figs. 4(a) and 4(b)] the position of the transmission minima under normal incidence follows the condition $\lambda_{\text{spp}} = p_x = p_y$, leading to $\lambda_{\min} = 622.6\,\text{nm}$ for air background and $\lambda_{\min} = 864.5\,\text{nm}$ for SiO_2 background.

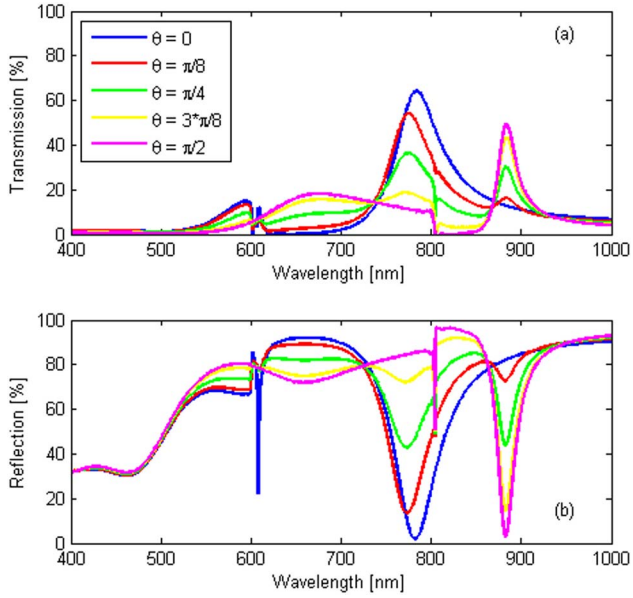

Fig. 3. (Color online) (a) Transmission and (b) reflection spectra as a function of the polarization angle θ ranging from 0 to $\pi/2$. Geometrical parameters are $p_x = 600\,\text{nm}$, $p_y = 800\,\text{nm}$, $a = 60\,\text{nm}$, and $w = 200\,\text{nm}$ (the structure is surrounded by air).

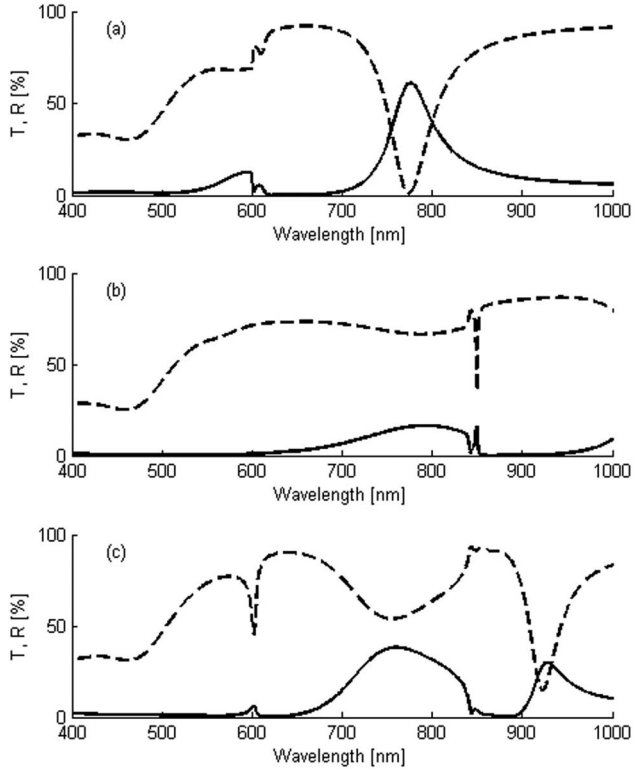

Fig. 4. Transmission (solid curve) and reflection (dashed curve) profiles for three different configurations: (a) metal patches in air, (b) embedded in SiO_2, and (c) over a SiO_2 substrate. Simulations have been performed with the same geometrical parameters $p_x = p_y = 600\,\text{nm}$, $a = 60\,\text{nm}$, and $w = 200\,\text{nm}$, with an input source linearly polarized along the x axis.

On the other hand, the presence of the semi-infinite substrate combines these results leading to the evidence of two forbidden transmission bands located around two slightly different wavelengths ($\lambda_1 = 623.6\,\text{nm}$ and $\lambda_2 = 881.7\,\text{nm}$). These bands mold the FP-like resonance shown in Fig. 1 (see the dotted curve). The analysis proves that physical and geometrical parameters can be optimized in order to engineer the spectral behavior of the actual structure, broadening the gap extension or modifying its spectral position.

In conclusion we have demonstrated that the spectral response of 2D arrays of gold patches exhibits forbidden bands whenever the effective wavelength of the unperturbed SPP of the air–metal or dielectric–metal interface matches the periodicity of the structure. Position, extension, and sharpness of such bands depend on the geometrical parameters of metal patches and on the optical properties of surrounding media. We have shown that squared arrays of gold patches are polarization insensitive, whereas transmission and reflection profiles for rectangular arrays of gold patches are strongly dependent on the polarization of the exciting field. Finally, we have studied transmission bands for array of gold patches over an SiO_2 substrate. The calculated positions of inhibited transmission bands are close to those obtained when the array is embedded in each constitutive medium of the complete system, i.e., air or SiO_2. These unique aspects pave the way for many new devices based on plasmonic resonances to be used in several applications where a specific polarization behavior is required, such as for patterned metal reflectors for thin film solar cells, achieving reflectivity values almost equal to 100%. At the same time, these features can also lead to the development of new polarization-sensitive optical filters, switches, and sensors operating in a wide optical range spanning from visible to infrared frequencies.

The authors acknowledge the Consorzio Interuniversitario dell'Italia Nordest per il Calcolo Automatico (CINECA) Award for the proposed project PlaNELA—Plasmonic Nanostructures for Enhanced Light Absorption 2010—for the availability of high-performance computing resources and support and also acknowledge the European Cooperation in Science and Technology (COST) action MP0702 on Towards Functional Sub-Wavelength Photonic Structures. They thank Dr. G. Erbacci and Dr. N. Varini for their technical support.

References

1. M. A. Vincenti, A. D'Orazio, M. Buncick, N. Akozbek, M. J. Bloemer, and M. Scalora, J. Opt. Soc. Am. B **26**, 301 (2009).
2. M. A. Vincenti, V. Petruzzelli, F. Prudenzano, A. D'Orazio, M. J. Bloemer, N. Akozbek, and M. Scalora, J. Nanophoton. **2**, 021851 (2008).
3. V. Marrocco, M. Grande, R. Marani, G. Calò, V. Petruzzelli, A. D'Orazio, T. Stomeo, M. De Vittorio, and A. Passaseo, in *International Conference on Transparent Optical Networks* (IEEE, 2010), paper Mo.C2.3.
4. T. W. Ebbesen, H. J. Lezec, H. F. Ghaemi, T. Thio, and P. A. Wolff, Nature **391**, 667 (1998).
5. F. J. Garcìa-Vidal, H. J. Lezec, T. W. Ebbesen, and L. Martìn-Moreno, Phys. Rev. Lett. **90**, 213901 (2003).
6. J. E. Kihm, Y. C. Yoon, D. J. Park, Y. H. Ahn, C. Ropers, C. Lienau, J. Kim, Q. H. Park, and D. S. Kim, Phys. Rev. B **75**, 035414 (2007).
7. Y. Xie, A. R. Zakharian, J. V. Moloney, and M. Mansuripur, Opt. Express **13**, 4485 (2005).
8. D. Pacifici, H. J. Lezec, H. A. Atwater, and J. Weiner, Phys. Rev. B **77**, 115411 (2008).
9. M. A. Vincenti, D. de Ceglia, M. Buncick, N. Akozbek, M. J. Bloemer, and M. Scalora, J. Appl. Phys. **107**, 053101 (2010).
10. E. D. Palik, *Handbook of Optical Constants of Solids* (Academic, 1985).
11. J. M. McMahon, J. Henzie, T. W. Odom, G. C. Schatz, and S. K. Gray, Opt. Express **15**, 18119 (2007).
12. http://www.thecomputationalphysicist.com/.